IEEE Access
Multidisciplinary | Rapid Review | Open Access Journal

Received November 23, 2018, accepted December 26, 2018, date of publication January 1, 2019, date of current version January 23, 2019.

Digital Object Identifier 10.1109/ACCESS.2018.2890435

Visible Light Communication-Based Vehicle-to-Vehicle Tracking Using CMOS Camera

TRONG-HOP DO AND MYUNGSIK YOO
School of Electronic Engineering, Soongsil University, Seoul 06978, South Korea

Corresponding author: Myungsik Yoo (myoo@ssu.ac.kr)

This work was supported by the Basic Science Research Program through the National Research Foundation of Korea, Ministry of Education, Science, and Technology, under Grant NRF-2018R1A2B6004371.

ABSTRACT This paper presents a visible light-communication-based vehicle-to-vehicle tracking system using a new positioning algorithm and modified version of the Kalman filter. In this system, LED head and tail lamps on the vehicles are used to transmit the positioning signals to other vehicles. Two CMOS dashboard cameras on each vehicle are used to receive these signals. From the geometric relationship between two cameras and the images of LEDs captured by these two cameras, the instantaneous position of the target vehicle can be determined, given that at least one LED of the target vehicle is in the view frame of the two cameras. The discrete positioning result always contains unavoidable errors, which consist of systematic errors caused by the CMOS rolling shutter artifact and the weak spatial separability of the sensor, and other random errors. The contribution of this paper is twofold. First, a new positioning algorithm with two compensation mechanisms is proposed to eliminate systematic errors. Second, a modified Kalman filter is proposed to filter out random errors to achieve a smooth and accurate tracking result for the vehicle position. The performance of the system is verified through simulations.

INDEX TERMS Visible light communication, vehicle, tracking, camera, Kalman filter.

I. INTRODUCTION

Intelligent transport systems (ITSs) are unarguably the future of transportation and traffic management, providing a safer, better informed, more coordinated driving experience for users along with other value-added services [1]–[4]. Many technologies have been proposed in recent years; however, there is still no standard or well-accepted technology suitable for the development of ITSs. This is not only due to the complexity of the system, but also the diversity of the applicable technologies to ITSs. There are two primary components of an ITS: vehicle communication and vehicle positioning. There are many candidate technologies for vehicle communication as well as vehicle positioning, but no technology has been shown to be significantly better than others. Integrating many technologies for all of the communication and positioning components also leads to issues of complexity and cost. However, in recent years a new technology has emerged, namely, camera based visible light communication (VLC) that has many advantages and is a potential key technology for ITSs.

The first advantage of VLC is the availability of the required hardware, resulting in a low cost implementation [5]–[8]. The primary hardware of a VLC are LEDs and cameras, used as transmitters and receivers, respectively. LEDs have been used in vehicles as front and tail lamps, and in particular, daytime running lamps, which are used to send simple signals to increase the conspicuity of the vehicle during daylight conditions. The use of high-resolution dashboard cameras has also become increasingly common in vehicles. The second advantage of VLC is its versatility. VLC can be used for vehicle communication, as well as vehicle positioning [9]–[12]. In other words, the implementation of this technology covers all of the required functions of an ITS, although the combination of VLC with other technologies may improve the system performance. In addition, VLC also has an advantage from the performance perspective. More specifically, one of the most challenging problems of vehicle communication is interference. There is no interference when using VLC due to its line-of-sight communication property. The performance in terms of the positioning of VLC has also

improved greatly due to the development of high-resolution cameras in recent years. Although the positioning accuracy provided by VLC is not as good as that of LIDAR, which is a very expensive technology, it is still superior to other affordable technologies such as GPS, WiFi, infrared, and ultra sound. For these reasons, VLC may be a key technology in future ITSs.

This study aims to use VLC to solve a single ITS problem: vehicle-to-vehicle (V2V) tracking. In the literature, the terminology 'tracking' is used to refer to a type of positioning in which consecutive discrete positioning results, estimated over time, are used to produce continuous tracking results of the vehicle position that tend to be more accurate than discrete positioning results. In other words, tracking provides an improvement over discrete positioning [13], [14].

In VLC based V2V positioning, LED head and tail lamps on the target vehicle are used to transmit positioning signals. Dashboard cameras on the estimating vehicles are used to capture the images of these LEDs. The LED images are then processed to determine the positions of the target vehicles. As VLC is a promising technology for V2V positioning, it has received considerable research attention. However, all existing research on this topic propose algorithms differing only slightly each other. Although some algorithms improve the performance compared with others, the results of these algorithms have a high degree of error variance due to the inherent property of discrete positioning. In this study, a VLC based V2V tracking system is used to improve the accuracy of discrete VLC based V2V positioning systems.

In the literature, most tracking systems are implemented using the Kalman filter. The problem with this is that the Kalman filter contains requirements that prevent it from being directly applicable to every system. The V2V positioning using a camera considered in this study is one such system. More specifically, the Kalman filter requires the errors of the system to have a white characteristic, zero mean, and constant variance. The errors in a camera-based VLC based V2V positioning system do not follow these rules because, besides random error, they also include systematic errors. These systematic errors include errors caused by rolling shutter artifacts of the CMOS sensor, which is currently the type of sensor used in almost all commercial cameras including dashboard cameras installed in vehicles. In addition, the weak spatial separability of the cameras at long distances is another source of systematic error. These systematic errors cause the error of our system to have varying and non-zero mean, varying variance, and non-white characteristic. Consequently, the direct application of the Kalman filter to our system would lead to undesirable results.

In this study, the systematic errors of the positioning system using camera-based VLC is reduced when using the proposed compensation methods. A modified version of the Kalman filter is proposed to filter out the remaining random error to achieve accurate and smooth tracking results of the vehicle position. The performance of the system is verified through simulations.

II. SYSTEM FUNDAMENTALS AND SOURCES OF SYSTEMATIC ERRORS

A. SYSTEM ARCHITECTURE

The architecture of a VLC based V2V tracking system is depicted in Fig. 1. The light from the LED lamps on the vehicles are modulated to transmit positioning signals, which may simply be the ID of these vehicles. In the simplest case, the positioning signals can be blinking patterns of LEDs that facilitate the detection of the vehicle and help differentiate them from other non-vehicle lights. The images of the LED lamps of the target vehicles are captured by two dashboard cameras installed on the windshield and processed by a CPU on the estimating vehicle. By using image processing, the coordinates of the LEDs in the images are obtained. Then the geometric relationship between the LED image coordinates and relative positions between two cameras are used to determine the position of the target vehicle relative to the estimating vehicle.

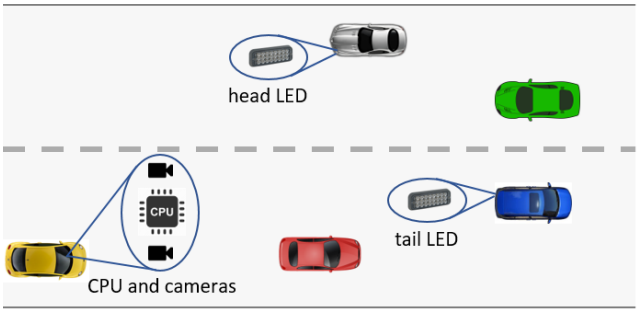

FIGURE 1. VLC based V2V positioning system.

B. BASICS OF THE COMPUTER VISION-BASED POSITIONING ALGORITHM AND TRACKING

1) POSITIONING USING THE COLLINEARITY CONDITION

All of the positioning algorithms using cameras are based on the pinhole camera model [15], which is shown in Fig. 2. There are two types of coordinates for the LEDs in this model: world and image.

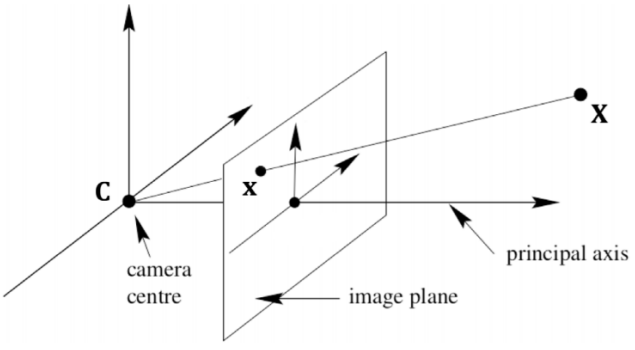

FIGURE 2. Pinhole camera model.

In this model, $\mathbf{x} = (x, y)$ is the image coordinate of the LED; $\mathbf{X} = (X, Y, Z)$ is the unknown world coordinate of

the LEDs, which can be considered as the position of the target vehicle; and $\mathbf{C} = (X_0, Y_0, Z_0)$ is the world coordinate of the camera on the estimating vehicle. The geometric relationship between these coordinates is given by the collinearity equations:

$$\begin{cases} x = -f \dfrac{R_{11}(X - X_0) + R_{12}(Y - Y_0) + R_{13}(Z - Z_0)}{R_{31}(X - X_0) + R_{32}(Y - Y_0) + R_{33}(Z - Z_0)} \\ y = -f \dfrac{R_{21}(X - X_0) + R_{22}(Y - Y_0) + R_{23}(Z - Z_0)}{R_{31}(X - X_0) + R_{32}(Y - Y_0) + R_{33}(Z - Z_0)}, \end{cases} \quad (1)$$

where f is the focal length of the lens and R_{ij} is the element at the i^{th} row and j^{th} column of the camera rotation matrix, R. In Eq. (1), the lens focal length is assumed to be known. Assuming that the pose of the camera can be obtained through some type of inertial sensor, the camera rotation matrix can be obtained. The LED image coordinates are obtained through image processing. Equation (1) can be transformed into a set of linear equations that can be solved using the linear least square method to obtain the three variables (X, Y, Z), which relate to the position of the target vehicle relative to the estimating vehicle.

2) TRACKING USING THE KALMAN FILTER

A Kalman filter is an optimal estimation algorithm used to estimate states, including the position and velocity, of the target vehicle from two inputs: predicted state and positioning result [13], [14]. Both inputs contain errors with different variances as described in Fig. 3. The Kalman filter includes two phases: predict and update. In the predict phase, a prediction is made based on the previous state and physical model of the system. In the update phase, the positioning results are obtained through a camera-based positioning algorithm. The optimal Kalman gain, which is a relative weight given to the prediction and positioning results, is calculated from the estimated error covariances of the prediction and positioning results. The optimal estimated state of the target vehicle is calculated from the optimal Kalman gain.

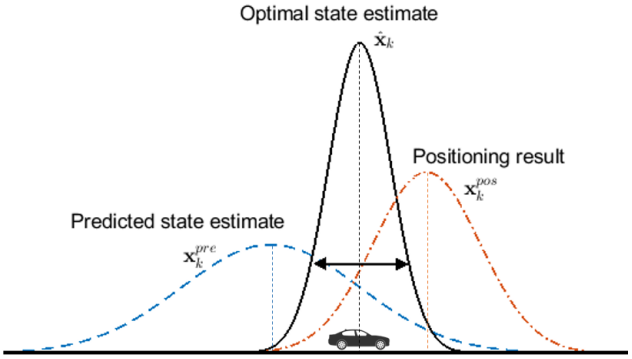

FIGURE 3. Kalman filter concept.

C. ERROR SOURCES IN POSITIONING AND TRACKING

1) POSITIONING ERROR CAUSED BY ROLLING SHUTTER ARTIFACT

The rolling shutter mechanism of the CMOS sensor is illustrated in Fig. 4. In the CMOS sensor, the scene is captured

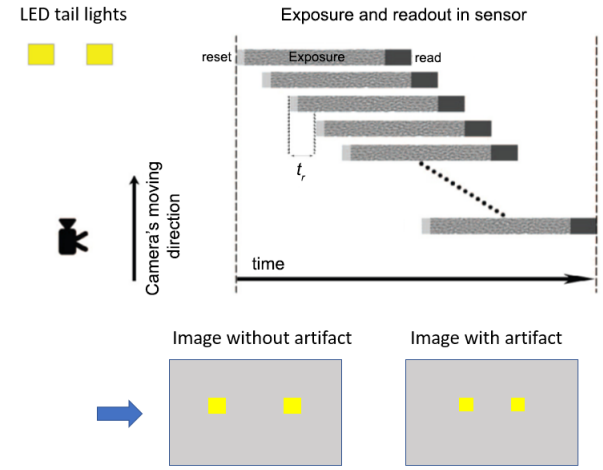

FIGURE 4. Rolling shutter mechanism and image artifact.

and read, row by row, in the sensor. The time required for the whole sensor to be read is called the readout time. Because of this mechanism, image artifacts appear if the camera is moving while capturing the image. If the camera is moving towards the LED tail lights, the LEDs appear in the captured image as if they are closer to the camera. After the LEDs are captured in the image, the two vehicles are still moving. Therefore, the vehicle position determined through an image with artifacts contain errors.

2) POSITIONING ERROR CAUSED BY THE WEAK SPATIAL SEPARABILITY OF THE IMAGE SENSOR

The accuracy of any camera-based positioning is greatly determined by the spatial separability of the image sensor, which varies depending on two factors: sensor resolution and camera perspective. It is clear that the higher the sensor resolution, the higher the spatial separability, and thus the higher the positioning accuracy. Regarding the camera perspective, the image of two LEDs would be more spatially separable in the image sensor when the difference between their perspectives to the camera is greater. In the case that two LEDs belong to two vehicles that have the same perspective as the camera as depicted in Fig. 5a, their images completely overlap and thus the same positioning results are obtained, which is incorrect since their real positions are different.

The overlapping problem can be dealt with by video and image processing techniques, which is outside the scope of this study. If two LEDs have different perspectives to the camera, the variations in the perspective differences depend on the positioning axis and distance between the LEDs and camera. It can be seen in Fig. 5b and 5c that the image sensors have better lateral spatial (i.e. across the street) separability compared with the longitudinal spatial (i.e. along the street) separability. The spatial separabilities in both axes are always lower at longer distance. In particular, the longitudinal spatial separability decreases substantially as the distance increases. As depicted in Fig. 5c, the two LEDs at long distances

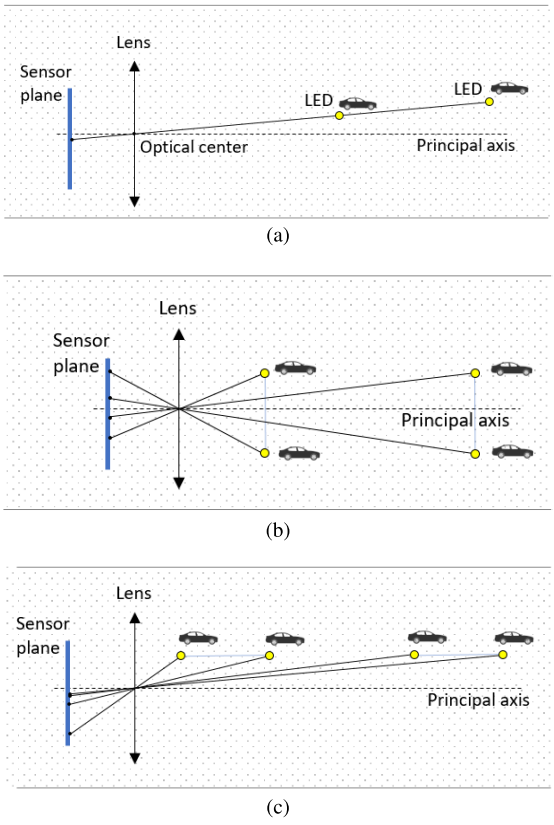

FIGURE 5. Spatial separability of the image sensor. (a) Overlapping images of two LEDs with the same perspective as the camera. (b) Lateral spatial separability of the image sensor at short and long distances. (c) Longitudinal spatial separability of the image sensor at short and long distances.

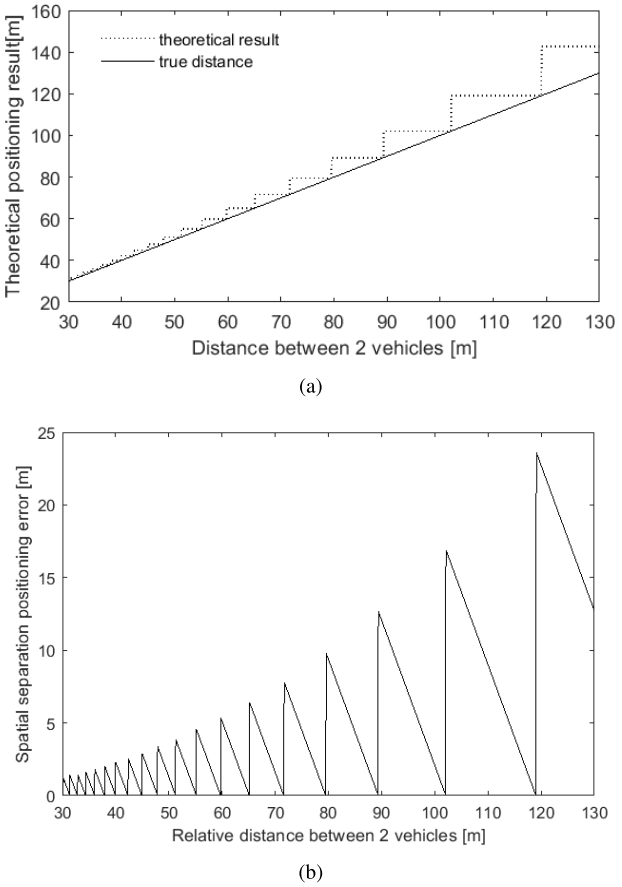

FIGURE 6. Theoretical longitudinal error caused by weak spatial separability. (a) Theoretical longitudinal positioning result. (b) Theoretical longitudinal positioning error caused by weak spatial separability.

are nearly indistinguishable in the image sensor and thus, the longitudinal positioning results, which are the estimated distances between the camera and two vehicles, are nearly identical.

As vehicles moves along the street, the relative position of the target vehicle changes. However, the target vehicle may still appear at the same position in the image sensor because of the weak longitudinal spatial separability of the image sensor.

As shown in Fig. 6a, there are intervals when the vehicles appear at the same position in the image sensor, resulting in the same positioning results indicated by the straight dotted line. Because of this behavior of the positioning result, the longitudinal positioning error would have a sawtooth pattern shown in Fig. 6b.

Since the longitudinal spatial separability of the image sensor decreases as the distance between two vehicles increases, the intervals where the positioning results remain the same get longer as the distance increases. This translates to the increased longitudinal positioning error, as shown in Fig. 6b.

3) TRACKING ERROR WHEN USING THE KALMAN FILTER

As mentioned previously, the Kalman filter was designed to deal with signals containing noise with specific characteristics: zero mean and white. The characteristic of

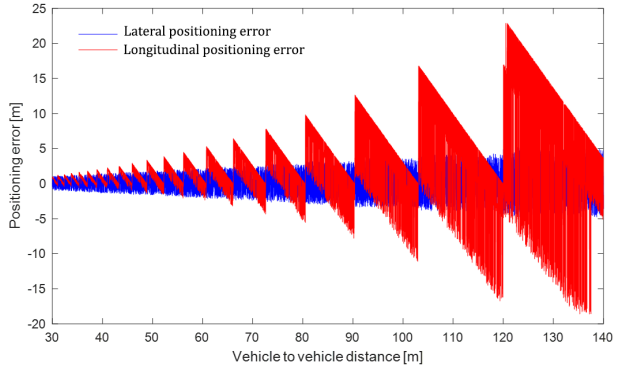

FIGURE 7. Characteristic of the positioning errors.

positioning errors are shown in Fig. 7. The positioning error does not have zero mean because of the systematic errors caused by the rolling shutter artifact and the weak spatial separability of the image sensor. Also, the positioning errors have repeated sawtooth patterns because of the systematic errors. When the relative speed and distances between vehicles increases, their impacts on the systematic errors increase and thus the variance of the errors increase. Consequently, the positioning errors do not have the white characteristic.

Therefore, applying the Kalman filter directly to the positioning results leads to unavoidable errors.

III. PROPOSED TRACKING SYSTEM

A. OVERALL ARCHITECTURE OF PROPOSED TRACKING SYSTEM

The proposed vehicle tracking system is illustrated in Fig. 8. In the error statistical collection step, the positioning system is tested and information regarding the acceleration of vehicles and positioning errors are obtained. Then, covariance of the positioning errors at different distances and the covariance of the acceleration of vehicles in normal driving conditions are calculated. The statistical information is then used in the Kalman filter equations.

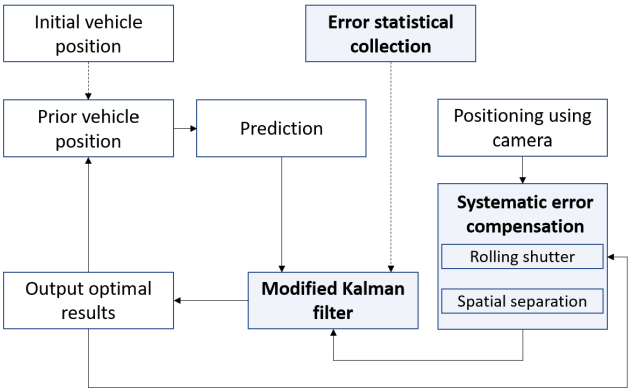

FIGURE 8. Proposed tracking system.

From the initial estimated vehicle position, the system performs a loop. In each round of the loop, the previous estimated vehicle position is used to predict the current vehicle position. On the other hand, the current position of the vehicle is also determined using the image captured by the camera. A systematic error compensation, which includes rolling shutter compensation and spatial separability compensation, is then applied to the positioning result. The predicted position and compensated camera-based positioning results are then fed to the modified Kalman filter to provide the optimal estimated state, including the position and relative speed of the target vehicle. The modified Kalman filter takes into account the differences in the error variances corresponding to different system parameters from the collected statistical error information. The optimal estimated position output is then provided as the prior vehicle position for the next round of the tracking loop. The optimal estimated state output is also used for systematic error compensation in the next round of the tracking loop.

B. POSITIONING USING TWO CAMERAS

Two cameras on the estimating vehicle are assumed to have the same angle. If we define (X_1, Y_1, Z_1) and (X_2, Y_2, Z_2) as the known world coordinates of the two cameras; (x_1, y_1) and (x_2, y_2) as the known image coordinates of a single vehicle LED on two images captured by the two cameras; and (X, Y, Z) as the unknown world coordinate of the LED on the target vehicle, a set of four linear equations can be formed as follows:

$$\begin{cases} x_1 = -f\dfrac{R_{11}(X-X_1)+R_{12}(Y-Y_1)+R_{13}(Z-Z_1)}{R_{31}(X-X_1)+R_{32}(Y-Y_1)+R_{33}(Z-Z_1)} \\ y_1 = -f\dfrac{R_{21}(X-X_1)+R_{22}(Y-Y_1)+R_{23}(Z-Z_1)}{R_{31}(X-X_1)+R_{32}(Y-Y_1)+R_{33}(Z-Z_1)} \\ x_2 = -f\dfrac{R_{11}(X-X_2)+R_{12}(Y-Y_2)+R_{13}(Z-Z_2)}{R_{31}(X-X_2)+R_{32}(Y-Y_2)+R_{33}(Z-Z_2)} \\ y_2 = -f\dfrac{R_{21}(X-X_2)+R_{22}(Y-Y_2)+R_{23}(Z-Z_2)}{R_{31}(X-X_2)+R_{32}(Y-Y_2)+R_{33}(Z-Z_2)}. \end{cases} \tag{2}$$

The equation set (2) has four equations with the three unknown variables (X, Y, Z) that can be solved by the linear least square method and thus the position of the target vehicle can be determined.

C. SYSTEMATIC ERROR COMPENSATION

1) ROLLING SHUTTER COMPENSATION

The concept of rolling shutter compensation is that every LED is captured at a different row in the image sensor and time lapses after the rolling shutter scans the first row of the image sensor. The two vehicles move a distance during this time. The proposed rolling shutter compensation is aimed at compensating for the displacements of the two vehicles. Rolling shutter compensation for vehicle to street lights positioning was introduced in [12]. In this study, this idea is applied to a vehicle-to-vehicle positioning system where both the estimating and target vehicles are moving, and a positioning algorithm that differs from [12] is employed.

Let $\Delta C(\Delta_X, \Delta_Y, \Delta_X)$ denote the displacement of the target vehicle relative to the estimating vehicle during the rolling shutter scanning time. The correct world coordinates of the LED in the target vehicle are $(X + \Delta_X, Y + \Delta_Y, Z + \Delta_Z)$.

$$\begin{cases} x_1 = -f\dfrac{R_{11}(X+\Delta_X-X_1)+R_{12}(Y+\Delta_Y-Y_1)+R_{13}(Z+\Delta_Z-Z_1)}{R_{31}(X+\Delta_X-X_1)+R_{32}(Y+\Delta_Y-Y_1)+R_{33}(Z+\Delta_Z-Z_1)} \\ y_1 = -f\dfrac{R_{21}(X+\Delta_X-X_1)+R_{22}(Y+\Delta_Y-Y_1)+R_{23}(Z+\Delta_Z-Z_1)}{R_{31}(X+\Delta_X-X_1)+R_{32}(Y+\Delta_Y-Y_1)+R_{33}(Z+\Delta_Z-Z_1)} \\ x_2 = -f\dfrac{R_{11}(X+\Delta_X-X_2)+R_{12}(Y+\Delta_Y-Y_2)+R_{13}(Z+\Delta_Z-Z_2)}{R_{31}(X+\Delta_X-X_2)+R_{32}(Y+\Delta_Y-Y_2)+R_{33}(Z+\Delta_Z-Z_2)} \\ y_2 = -f\dfrac{R_{21}(X+\Delta_X-X_2)+R_{22}(Y+\Delta_Y-Y_2)+R_{23}(Z+\Delta_Z-Z_2)}{R_{31}(X+\Delta_X-X_2)+R_{32}(Y+\Delta_Y-Y_2)+R_{33}(Z+\Delta_Z-Z_2)}, \end{cases} \tag{3}$$

Then, Eq. (2) is rewritten as (3), as shown at the bottom of the previous page.

The coordinate ΔC now needs to be calculated. Assuming that t_r is the row readout time of the image sensor and r_i is the row where the LED appears in the image sensor, the elapsed time, Δt, since the beginning of the frame to the time when the LED is captured is given by:

$$\Delta t = t_r \times r_i. \tag{4}$$

The displacement of the target vehicle can be calculated given that the relative speed, v, between two vehicles is known as:

$$\Delta C = \Delta t \times v. \tag{5}$$

In the proposed tracking system, the relative speed between vehicles is estimated using the modified Kalman filter.

2) SPATIAL SEPARABILITY COMPENSATION

Given the system parameters, which include the pose angle of the cameras, resolution of the cameras, and focal length of the lens, the theoretical positioning result shown in Fig. 6a can be simulated and calculated beforehand. From the theoretical positioning results, the theoretical positioning error caused by the weak spatial separability of the image sensor can be calculated as described in Fig. 6b.

Suppose that $\mathbf{x}$ is the positioning result, the weak spatial separability positioning error can be compensated using:

$$\mathbf{x}^{pos} = \mathbf{x} - \tau_{\mathbf{x}}, \tag{6}$$

where $\mathbf{x}^{pos}$ is the compensated positioning result, and $\tau_{\mathbf{x}}$ is the theoretical error at the relative position $\mathbf{x}$ obtained beforehand. After compensated, the positioning result contains only random errors which can be filtered out using Kalman filter.

D. MODIFIED KALMAN FILTER

At time k, the state, which contains the true information regarding the position and velocity of the target vehicle along the lateral and longitude axes, is described by a vector:

$$\mathbf{x}_k = \begin{bmatrix} X_k \\ Y_k \\ \dot{X}_k \\ \dot{Y}_k \end{bmatrix}, \tag{7}$$

where X and Y are the lateral and longitude positions of the target vehicle, respectively; and $\dot{X}$ and $\dot{Y}$ are the velocities of the target vehicle along the lateral and longitude axes, respectively.

The prediction of $\mathbf{x}_k$ is denoted by $\mathbf{x}_k^{pre}$, the positioning result of $\mathbf{x}_k$ is denoted by $\mathbf{x}_k^{pos}$, and the optimal estimated result of $\mathbf{x}_k$ obtained through the Kalman filter is denoted by $\hat{\mathbf{x}}_k$.

In the prediction phase, the current state of the target vehicle, $\mathbf{x}_k^{pre}$, can be calculated from the previous optimal estimated state, $\hat{\mathbf{x}}_{k-1}$, using the physical laws of motion, and is given by:

$$\mathbf{x}_k^{pre} = \mathbf{F}_k \hat{\mathbf{x}}_{k-1} \tag{8}$$

where $\mathbf{F}_k$ is the state-transition model given by

$$F = \begin{bmatrix} 1 & 0 & \Delta t & 0 \\ 0 & 1 & 0 & \Delta t \\ 0 & 0 & 1 & 0 \\ 0 & 0 & 0 & 1 \end{bmatrix}. \tag{9}$$

Let $\mathbf{P}_{k-1}$ denote the error covariance of the previous optimal estimated state $\hat{\mathbf{x}}_{k-1}$, and $\mathbf{P}_k^{pre}$ denote the error covariance of the current prediction $\mathbf{x}_k^{pre}$. Then $\mathbf{P}_k^{pre}$ can be estimated by:

$$\mathbf{P}_k^{pre} = \mathbf{F}\mathbf{P}_k\mathbf{F}^{\mathbf{T}} + \mathbf{Q}, \tag{10}$$

where $\mathbf{Q}$ is the covariance of the process noise given by:

$$\mathbf{Q} = \begin{bmatrix} \frac{\Delta t^4}{4} & \frac{\Delta t^3}{2} \\ \frac{\Delta t^3}{2} & \Delta t^2 \end{bmatrix} \sigma_a^2, \tag{11}$$

where σ_a^2 is the variance of the acceleration of vehicles in normal driving conditions obtained in the error statistical collection step.

In the update phase, the positioning pre-fit residual $\mathbf{x}_k^{res}$ is calculated using:

$$\mathbf{x}_k^{res} = \mathbf{x}_k^{pos} - \mathbf{H}\mathbf{x}_k^{pre}, \tag{12}$$

where $\mathbf{H}$ is the observation model that maps the true state $\mathbf{x}_k$ to the positioning result $\mathbf{x}_k^{pos}$:

$$\mathbf{H} = \begin{bmatrix} 1 & 0 & 0 & 0 \\ 0 & 1 & 0 & 0 \end{bmatrix}. \tag{13}$$

The covariance of the positioning pre-fit residual, denoted as $\mathbf{S}_k$, is given by:

$$\mathbf{S}_k = \mathbf{R}_{\mathbf{x}_k^{pre}} + \mathbf{H}_k\mathbf{P}_k^{pre}\mathbf{H}^{\mathrm{T}}, \tag{14}$$

where $\mathbf{R}_{\mathbf{x}_k^{pre}}$ is the covariance of the positioning error expected at the current state of the target vehicle obtained in the error statistical collection step.

As explained previously, the problem with the current Kalman filter is that the errors need to be white and have zero mean to be filtered out effectively. By applying the systematic error compensation, the positioning error will only include a random error which has zero mean. However, the covariance of the positioning error $\mathbf{R}_{\mathbf{x}_k^{pre}}$ do not remain the same at different distances. The reason is that the sources of random positioning errors includes the errors in the LED image coordinate detection and camera angle measurements. While the LED detection and camera angle measurement errors have the same variance at any time, their effect on the positioning error increases as the distance between two vehicles increases. Consequently, the covariance of the positioning error $\mathbf{R}_{\mathbf{x}_k^{pre}}$ increases as the distance increases.

In the literature, the positioning errors at all distances are collected to yield a single covariance $\mathbf{R}$, which is a constant for a specific positioning system. In this paper, the moving covariances of positioning errors are collected at all distances beforehand. When the system is running, the covariance of

positioning errors $\mathbf{R}_{\mathbf{x}_k^{pre}}$ corresponding to the current predicted state $\mathbf{x}_k^{pre}$ is used to calculate the covariance of the positioning pre-fit residual $\mathbf{S}_k$ in Eq. (14) with higher accuracy compared to that of using a constant covariance $\mathbf{R}$.

The covariance of the positioning pre-fit residual $\mathbf{S}_k$ is then used to calculate the Kalman gain:

$$\mathbf{K}_k = \mathbf{P}_k^{pre}\mathbf{H}^{\mathrm{T}}\mathbf{S}_k^{-1}. \tag{15}$$

Then, the optimal estimated state of the target vehicle is given by:

$$\hat{\mathbf{x}}_k = \mathbf{x}^{pre} + \mathbf{K}_k\mathbf{x}_k^{res}. \tag{16}$$

The error covariance of the current optimal estimated state, denoted as $\hat{\mathbf{x}}_k$, is given by:

$$\mathbf{P}_k = (\mathbf{I} - \mathbf{K}_k\mathbf{H})\mathbf{P}^{pre}. \tag{17}$$

IV. SIMULATION

A. SIMULATION ENVIRONMENT

The simulations are conducted with parameters described in Table 1.

TABLE 1. Simulation environment.

Parameter	Value
Sensor physical size	$36 \times 24\,(mm^2)$
Sensor resolution	1920×1080 (pixels)
Lens focal length	$35(mm)$
Frame per second	$30(fps)$
Readout time	$0.03(cm^2)$
Exposure time	$1/2000(s)$
LED size	$10 \times 10\,(cm^2)$
Inter-distance between 2 cameras	$100\,(cm)$
Height of cameras	$1.2\,(m)$
Height of LEDs	$0.6\,(m)$
Vehicle speed	0 to $100(km/h)$
Speedometer error	0 to 10 (%)
Interdistance between 2 vehicles	5 to $300(m)$
Simulation time	$10(s)$

B. SIMULATION PROCEDURE

The simulation procedure is illustrated in Fig. 9. Firstly, the vehicles with random positions, velocities, and acceleration are initialized. Given the relative positions of the vehicles and cameras and other parameters, the images of the LEDs can be replicated. The pixel coordinates of the LEDs are calculated using the pinhole camera model. The calculated pixel values of the LEDs are based on the LED luminance and camera exposure setting [16]. It is assumed that there is no object in the background. The LED images are then processed to detect the positions of the LEDs. The proposed tracking system is then applied to obtain the positions and velocities of the vehicles. The accuracy of the tracking result is calculated. The positions of the vehicles are then changed given the velocities set at the beginning of the simulation. It is also assumed that there are random changes in the accelerations and directions of the vehicles. The images of the LEDs in the new positions are replicated and the simulation continues. The system runs for 10 s during the simulation, after which, the simulation stops, and the performance of the tracking system is evaluated.

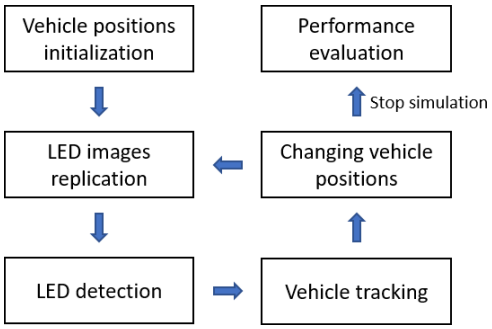

FIGURE 9. Simulation procedure.

The positioning error is the combination of three types of errors: rolling shutter (RS) error, spatial separability (SS) error, and random error. The RS error is caused by the movement of the vehicles, and thus is only dependent on the relative speed between two vehicles. On the other hand, the SS error is caused by the weak longitudinal spatial separability of the sensor and thus is only dependent on the distance between two vehicles. Therefore, to show the effect of the relative speed between two vehicles on the RS error, a simulation was conducted with variations in the relative speed between two vehicles and a fixed distance between them. To show the effect of the distance between two vehicles on the SS error, a simulation was conducted with variations in the distance between two vehicles and a fixed relative speed between them.

It is important to note that the positioning error includes the longitudinal and lateral errors. Since the longitudinal error is much more severe than the lateral error, only the longitudinal errors (i.e., the estimated distance errors) are shown in the simulation results.

C. SIMULATION RESULT

1) DISTANCE ERROR AT DIFFERENT RELATIVE SPEED AND FIXED DISTANCE

In this simulation, the relative speed ranges from -50 to 50 m/s, with a fixed distance between the two vehicles of 30 m. Note that in the simulation, the target vehicle can move in the same or opposite direction to the estimating vehicle. Even when two vehicles move in the same direction, the velocity of the target vehicle can be less or greater than that of the estimating vehicle. Therefore, the relative velocity of the target vehicle may range widely, either negative or positive. The results are shown in Fig. 10. Since the

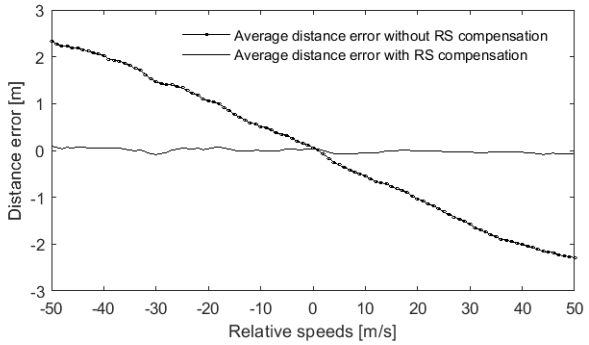

FIGURE 10. Distance error at different relative speed and fixed distance.

distance between two vehicles is fixed, the SS error is fixed, and thus the change in the distance error is due to the RS error. The estimated distance error is completely dependent on the relative speed. A positive distance error leads to a larger estimated distance compared with the true distance. A negative distance error leads to a smaller estimated distance compared with the true distance. It can also be seen in Fig. 10 that the rolling shutter compensation effectively eliminates the RS error at all relative speeds.

2) DISTANCE ERROR AT DIFFERENT DISTANCES AND FIXED RELATIVE SPEED

The estimated distance error at different distances between two vehicles is shown in Fig. 11a. In this simulation, the relative speed between two vehicles is set to 30 m/s. The distance error is composed of the RS, SS, and random errors.

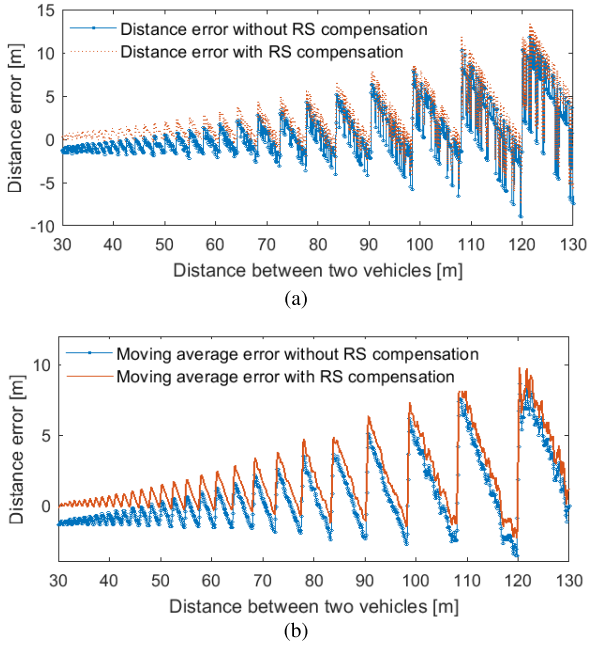

FIGURE 11. Error caused by rolling shutter artifact. (a) Distance error caused by rolling shutter at different distances. (b) Moving average distance error caused by rolling shutter at different distances.

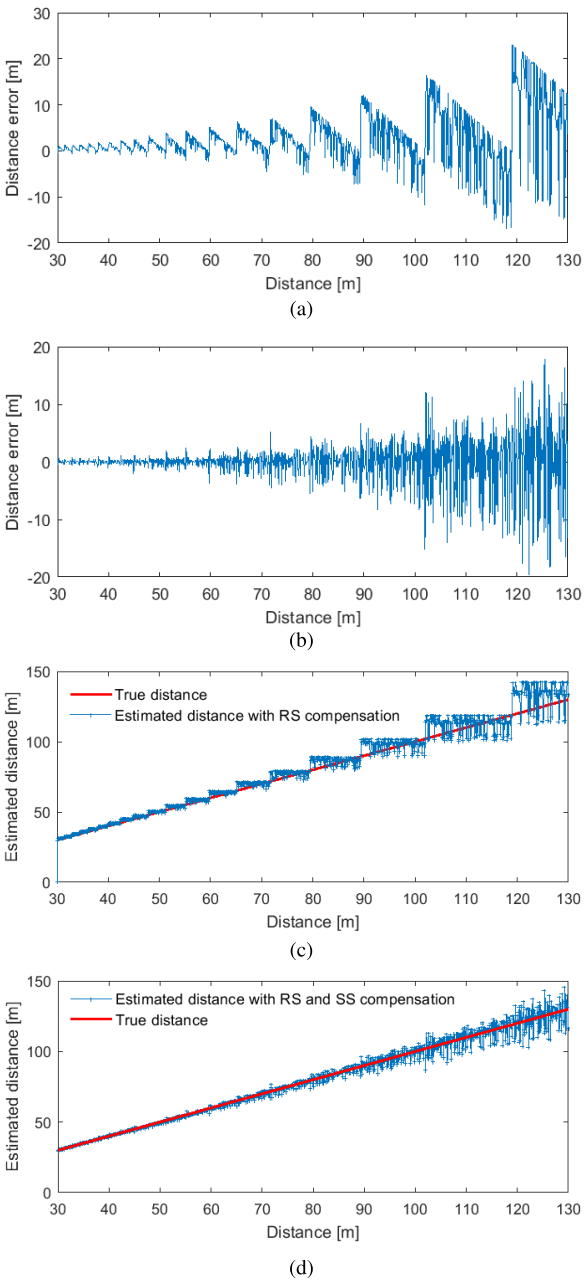

FIGURE 12. Positioning with RS and SS compensation at different distances. (a) Distance error with RS compensation and without SS compensation at different distances. (b) Distance error with both RS and SS compensation at different distances. (c) Estimated distance with RS compensation and without SS compensation at different distances. (d) Estimated distance with both RS and SS compensation at different distances.

Note that at a relative speed of 30 m/s, the RS error leads to lower estimated distances compared with the true distances. At short distances of up to 50 m, the RS error is greater than the SS and random errors, leading to a distance error without RS compensation well below that with RS compensation, as shown in Fig. 11a.

The SS error component leads to sawtooth pattern in the distance error as the distance increases. The random

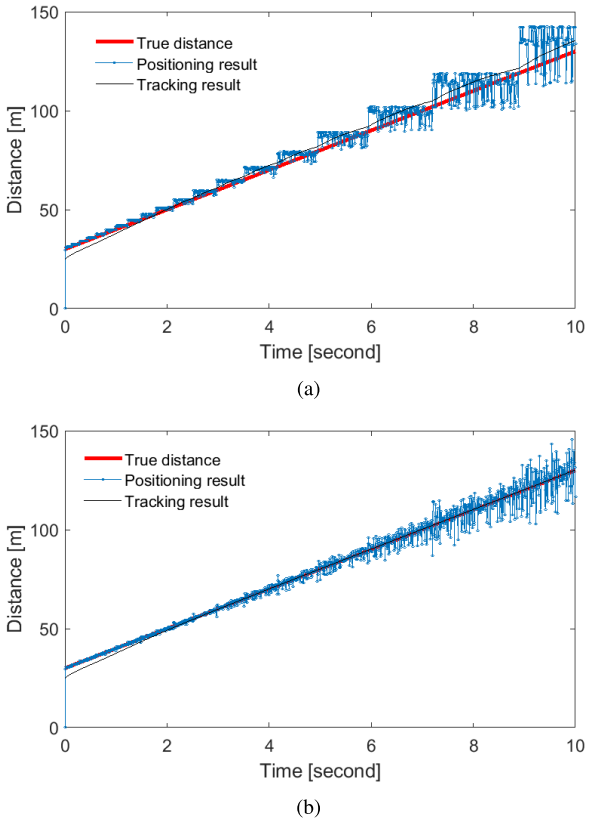

FIGURE 13. Tracking with and without error compensation. (a) Tracking without RS and SS error compensation. (b) Tracking with RS and SS error compensation.

error leads to the distance error fluctuating around the local mean. When the distance increases, the SS and random errors dominate the RS error, confusing the line plot of the distance errors with and without RS compensation. By calculating the moving average of the distance error, the random error component is essentially removed and the RS and SS error components can be revealed, as shown in Fig.11b.

3) SPATIAL SEPARABILITY ERROR COMPENSATION

In this simulation, the distances between two vehicles ranges from 30 to 130 m. The relative speed is fixed to 30 m/s. However, the RS compensation is applied to all positioning results. In Fig. 12a, the SS compensation is not applied as the distance error is composed of SS and random errors. In Fig. 12b, both RS and SS compensation is applied and thus only the random error component remained. It can be seen that the distance error in Fig. 12b has a zero mean and increasing variance with distance.

Another view of the effectiveness of the SS compensation is shown in Fig. 12c and 12d. In Fig. 12c, the estimated distance with SS error does not fluctuate around the true distance. By applying SS compensation, the estimated distance fluctuates around the true distance at all distances, as shown in Fig. 12d.

4) PERFORMANCE OF PROPOSED TRACKING SYSTEM

By applying RS and SS compensation, the systematic error components are removed from the positioning result. However, the estimated distance error is still high due to random errors. As shown in Fig. 12b, the distance error reaches 20 m as the distance between two vehicles is greater than 120 m. To filter out this random error, the Kalman filter is applied to the compensated positioning result and the results are shown in Fig. 13. In this simulation, the average relative speed between two vehicles is 30 m/s and the two vehicles are assumed to move within 10 s. In Fig. 13a, Kalman filter is applied without RS and SS compensation and thus the tracking result contains errors. In Fig. 13b, the modified Kalman filter is applied with RS and SS compensation and thus the tracking result has a much greater accuracy.

V. CONCLUSION

This paper proposes a vehicle-to-vehicle tracking system based on visible light communication using a CMOS sensor camera. The contribution of this study is twofold. First, a complete positioning system using two cameras is proposed. In this positioning system, systematic errors including rolling shutter artifact error and weak spatial separability error are effectively removed by the proposed compensation methods. Second, the Kalman filter is modified to deal with the changing variance of positioning errors. The effectiveness of the proposed tracking system is verified through simulation. The simulation results show that the tracking system can significantly improve the accuracy of the discrete positioning result.

REFERENCES

[1] G. Dimitrakopoulos and P. Demestichas, "Intelligent transportation systems," *IEEE Veh. Technol. Mag.*, vol. 5, no. 1, pp. 77–84, Mar. 2010.
[2] P. Papadimitratos, A. De La Fortelle, K. Evenssen, R. Brignolo, and S. Cosenza, "Vehicular communication systems: Enabling technologies, applications, and future outlook on intelligent transportation," *IEEE Commun. Mag.*, vol. 47, no. 11, pp. 84–95, Nov. 2009.
[3] Y. Zhao, "Mobile phone location determination and its impact on intelligent transportation systems," *IEEE Trans. Intell. Transp. Syst.*, vol. 1, no. 1, pp. 55–64, Mar. 2000.
[4] A. Amini, R. M. Vaghefi, J. M. de la Garza, and R. M. Buehrer, "Improving GPS-based vehicle positioning for intelligent transportation systems," in *Proc. IEEE Intell. Vehicles Symp.*, Jun. 2014, pp. 1023–1029.
[5] J.-H. Yoo, J.-S. Jang, J. K. Kwon, H.-C. Kim, D.-W. Song, and S.-Y. Jung, "Demonstration of vehicular visible light communication based on LED headlamp," *Int. J. Automot. Technol.*, vol. 17, no. 2, pp. 347–352, 2016.
[6] T. Yamazato *et al.*, "Image-sensor-based visible light communication for automotive applications," *IEEE Commun. Mag.*, vol. 52, no. 7, pp. 88–97, Jul. 2014.
[7] M. Kinoshita *et al.*, "Motion modeling of mobile transmitter for image sensor based I2V-VLC, V2I-VLC, and V2V-VLC," in *Proc. Globecom Workshops (GC Wkshps)*, Dec. 2014, pp. 450–455.
[8] I. Takai, T. Harada, M. Andoh, K. Yasutomi, K. Kagawa, and S. Kawahito, "Optical vehicle-to-vehicle communication system using LED transmitter and camera receiver," *IEEE Photon. J.*, vol. 6, no. 5, Oct. 2014, Art. no. 7902513.
[9] S.-H. Yu, O. Shih, H.-M. Tsai, N. Wisitpongphan, and R. Roberts, "Smart automotive lighting for vehicle safety," *IEEE Commun. Mag.*, vol. 51, no. 12, pp. 50–59, Dec. 2013.
[10] R. Roberts, P. Gopalakrishnan, and S. Rathi, "Visible light positioning: Automotive use case," in *Proc. IEEE Veh. Netw. Conf. (VNC)*, Dec. 2010, pp. 309–314.

[11] M. S. Ifthekhar, N. Saha, and Y. M. Jang, "Stereo-vision-based cooperative-vehicle positioning using OCC and neural networks," *Opt. Commun.*, vol. 352, pp. 166–180, Oct. 2015.
[12] T. H. Do and M. Yoo, "Visible light communication based vehicle positioning using LED street light and rolling shutter CMOS sensors," *Opt. Commun.*, vol. 407, pp. 112–126, Jan. 2018.
[13] R. G. Brown and P. Y. Hwang, *Introduction to Random Signals and Applied Kalman Filtering*, vol. 3. New York, NY, USA: Wiley. 1992.
[14] P. J. T. H. Venhovens and K. Naab, "Vehicle dynamics estimation using Kalman filters," *Vehicle Syst. Dyn.*, vol. 32, nos. 2–3, pp. 171–184, 1999.
[15] R. Hartley and A. Zisserman, *Multiple View Geometry in Computer Vision*, 2nd ed. Cambridge, U.K.: Cambridge Univ. Press, 2004.
[16] T.-H. Do and M. Yoo, "Performance analysis of visible light communication using CMOS sensors," *Sensors*, vol. 16, no. 3, p. 309, 2016.

TRONG-HOP DO received the B.Sc. degree in mathematics and computer science from the University of Science, Vietnam National University Ho Chi Minh City, Ho Chi Minh City, Vietnam, in 2009, and the Ph.D. degree in information and telecommunication from Soongsil University, Seoul, South Korea, in 2015. He is currently a Postdoctoral Researcher with the School of Electronic Engineering, Soongsil University. His current research interests include wireless sensor networks, visible light communication, and vehicle communication and sensing.

MYUNGSIK YOO received the B.S. and M.S. degrees in electrical engineering from Korea University, Seoul, South Korea, in 1989 and 1991, respectively, and the Ph.D. degree in electrical engineering from The State University of New York at Buffalo, Buffalo, NY, USA, in 2000. He was a Senior Research Engineer with the Nokia Research Center, Burlington, MA, USA. He is currently a Full Professor with the School of Electronic Engineering, Soongsil University, Seoul. His current research interests include visible light communications, optical networks, sensor networks, and Internet protocols.